Synthesis, Characterization and Molecular Docking of Statins Rational Drug Design Approach

Pravin Kumar Singh*[1,2], Saravanan K*[1], Prabhash Nath Tripathi[3], Omkar Singh[4]

[1]Faculty of pharmacy, Bhagwant University, Ajmer, Rajasthan, India

[2]Jubilant Biosys Limited, Noida, Uttar Pradesh, India

[3]Department of Pharmaceutical Technology, Centre for Chemical Research and Development (CCRD), Meerut Institute of Engineering and Technology, Meerut

[4] Rahul Sankrityayan College of Pharmacy, Jaigahan, Azamgarh, UP.

Abstract

The practice of bioisosteres in drug discovery is a well-accepted designing concept that has illustrated utility as an approach to resolve a broad range of complications that may affect candidate optimization, development and robustness. In this article, the application of isosteric replacement is explored in a fashion that well defined on the development of practical solutions to problems that are experience in typical drug optimization and designing. The role of bioisosteres to affect inherent potency, selectivity, influence conformation and solve troubleshoots associated with drug feasibility, including P-glycoprotein recognition, modulating basicity, solubility, and lipophilicity and as well as to address issues associated with metabolism and toxicity are used as the underlying theme to capture a spectrum of creative applications of structural emulation in the designing of drug candidates. The imidazole scaffold represents important structural subunits for the discovery of new drug candidates. The demonstration that any molecule contains the imidazole core scaffold contains three carbon atoms, and two nitrogen with electronic-rich characteristics responsible for readily binding with a variety of enzymes, proteins, and receptors compared to the other heterocyclic rings, giving rise to a huge number of biologically active synthetic products, with a wider range therapeutic activities. Herein, we represent a thorough overview of the current research status of imidazole-based compounds with a wide variety of biological activities including anti-cancer, anti-microbial, anti-inflammatory, HMG-CoA reductase inhibitors and their potential mechanisms. This possesses a discourse binding pocket that is acknowledge by the imidazole scaffold in a common interrelated domain, describe the huge number of drugs contain imidazole substructure such as etomidate, eprosartan, metronidazole among many others.

Keywords: Imidazole scaffold, HMG-CoA reductase, statin

Introduction

Cardiovascular disease (CVDs) hits approximately 17.9 million lives each year. This increase in number shows the concern related to CVDs. According to most of the reported literature, high plasma level of cholesterol is one of the severe risk factors for CVDs. Hence it seems necessary to modulate the lipid profile using appropriate strategies. 3-Hydroxy-3-methylglutaryl coenzyme A (HMG-COA) reductase enzyme act by inhibiting the rate limiting step in cholesterol biosynthesis i.e. conversion process of HMG-CoA to mevalonate. Therefore, it is recognized as the efficient target for successful cholesterol-lowering medicines. Statins are similar to natural substrates of the HMG-CoA reductase, competing with a substrate for the enzyme active site. Thus inhibiting the enzyme with statins prevents endogenous cholesterol production. As per literature reports, other such secondary mechanism of statins is through the inhibition of hepatic B100 Apo lipoprotein, which leads to a decrease in the synthesis and secretion of triglyceride. Hence, statins and its derivatives are the finest and most efficient candidates to inhibit HMG-CoA. Statins has emerged as the first-line therapy to prevent atherosclerotic cardiovascular disease for their ability to enhance the clearance of plasma low-density lipoproteins. Due to their broad range of pleiotropic effects, statins and its derivatives are evident as promising candidates for treatment of other diseases too. Atherosclerosis and atherosclerosis associated diseases such as cerebrovascular, coronary, and peripheral vascular diseases are accelerated by the presence of Hyperlipidemia. The main causes hyperlipidemia of unusual rise in cholesterol level, the consequence of an unhealthy lifestyle such as taking a high-fat diet and other lifestyle factors like being overweight, smoking, heavy alcohol use, and lack of exercise. Other factors include pregnancy, diabetes, kidney disease, and an under active thyroid gland. For the treatment of this chiefly involve the use of the drugs mainly identified as statins. In general, the drugs involved in the management of hyperlipidemia are classified as follows: Lovastatin, Simvastatin, Rosuvastatin, Atorvastatin, Pravastatin, choletyramine, Colestipol, Fenofibrates, Gemfibrozil, Nicotinic acid, Ezetimibe, Gugulipid etc.

2. Objectives

2.1 Hypertension

This is a long-term medical state in which the blood pressure in the arteries is constantly raised. Long-term high blood pressure is a key risk factor for coronary artery disease, heart failure, stroke, vision loss, peripheral vascular disease, and chronic kidney disease. Hypertension is often called "the silent killer" because it generally has no symptoms until serious complications developed. Hypertension is classified into primary (essential) and secondary HT. Around 90–95% of cases are primary HT arising because of nonspecific lifestyle as well as genetic factors. Lifestyle factors that increase the risk include high salt intake, smoking, excess body weight, and intake of alcohol. The other 5-10% of cases is regarded as secondary HT, which happens due to an identifiable or known cause, for instance narrowing of the kidney arteries, chronic kidney disease, the use of birth control pills, or an endocrine disorder. Blood pressure is articulated by measurement of the systolic and diastolic pressures i.e. the maximum and minimum pressures, correspondingly. Regular blood pressure at rest is within the range of 100–140 mmHg systolic and 60–90 mmHg diastolic. High blood pressure is evident if the resting blood pressure is

persistently at or above 140/90 mmHg for most adults.

2.2 Antihypertensive Drugs

As arterial pressure is a product of cardiac output and peripheral vascular resistance, it may be lowered by the action of the drug on either the peripheral resistance or cardiac output, or both. Drugs may be reduced cardiac output by either inhibiting myocardial contractility or decreasing ventricular filling pressure. Reduction in ventricular filling pressure may be achieved by action on the venous tone or on blood volume via renal effect. Drugs can reduce peripheral resistance by acting on smooth muscle to relaxation of resistance vessel or by interfering with the activity of systems that produced constriction of resistance vessels (e.g., the sympathetic nervous system).

2.3 HMG-CoA (HMG-CoA) Reductase Inhibitor (Statins)

These are the major drugs for the treatment or management of Hyperlipidemia, also called as HMG-CoA (HMG-CoA) Reductase Inhibitors e.g., Atorvastatin, Lovastatin, Fluvastatin, Pravastatin, Simvastatin and Rosuvastatin. Among the statins group of drugs, simvastatin was selected for the purpose of a new drug delivery formulation because of the following reasons. Simvastatin is a BCS class-II drug, and its oral absorption is dissolution rate-limited. It is employed to alleviate primary dyslipidemia and hypercholesterolemia. It is a specific and potent competitive inhibitor of HMG-CoA (3-hydroxy-3-methyl-glutarylcoenzymeA) reductase enzyme, which acts as a rate-limiting step in cholesterol biosynthesis in the liver. It also stimulates the hepatic low-density lipoprotein (LDL) receptors, hence increases the breakdown of LDL. Simvastatin, at gastric pH, is stable and remains in a unionized state. However, at intestinal pH, it gets ionized due to which gastrointestinal tract (GIT) absorption is reduced, resulting in low bioavailability. It also has an extensive hepatic first-pass metabolism (FPM) in the liver, which results in low oral bioavailability. The absolute oral bioavailability of simvastatin is ≤ 5%. Around 13% is excreted in urine and 60% infection in unabsorbed form. Drug delivery through oral buccal mucosa is an extremely complicated task, mainly when the drug is poorly soluble in water and has especially low systemic availability when administered orally. Buccal delivery systems can be utilized for both local as well as systemic delivery of drugs.

3. Results and Discussion

3.1 Designing consideration

By consideration of the reported literature, the known moiety like atorvastatin and rosuvastatin was strapped to a substituted imidazole nucleus within hybrid pharmacophore skeleton with the aim of developing multi-targeted ligands with the ability to inhibit AChE coenzyme-A as shown in figure 1.
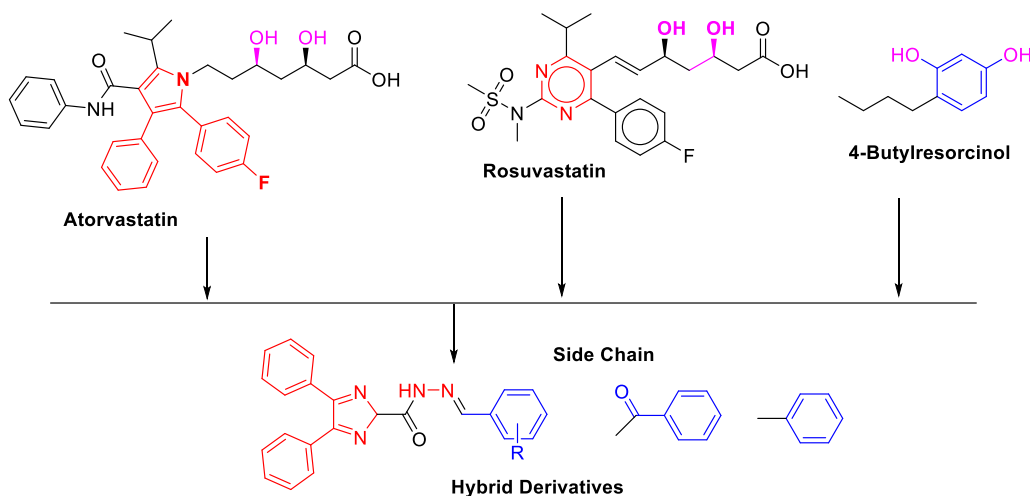
Figure 1. Designing strategy for the target conpounds

3.2 Chemistry

The scaffold 4 and its derivatives, **5a-e**, **6a-b** & **7a-d** were prepared using sequence described in scheme 1. Benzil **(1)** is reacted with ethyl 2-amino-2-oxoacetate **(2)** in the presence of ammonium acetate and ethanol at reflux temperature to give the 4,5-diphenyl-2H-imidazole ester **(3)**. Then, intermediate **(3)** refluxed with hydrazine in the absolute ethanol to afford the hydrazine carboxamide key intermediate **(4)**. The compound **(4)** reacted with the various substituted aldehydes generated the Schiff base (**5a, 5b, 5c, 5d**). As shown in scheme 2, in another reaction, intermediate **4** was reacted with various aromatic halides to give compounds (**6a, 6b, 6c**) in the presence of anhydrous potassium carbonate (K_2CO_3) at room temperature for 16 h. Compound **4** was further treated with benzoic acid in the presence of HATU, DIPEA & DMF to afford the compound (**7a, 7b, 7b, 7d**). Preliminary identification of derivatives was verified by Dragendroff test on TLC (Thin layer chromatography). These final compounds were purified by column chromatography to get the pure compounds with 60-84% yield. Further, the synthesized derivatives were established using the state of art spectroscopy. The structures of the compounds were confirmed by spectroscopy (FT-IR, ^{1}H NMR and ^{13}C NMR) and elemental analysis.

The ^{1}HNMR spectrum confirmed the formation of compound **2**, as evidence by the appearance of a diaryl proton peak at 7.43 ppm. The diagnostic peaks of the hydrazine (-$NHNH_2$) group of compound 4 appeared at ppm respectively. Furthermore, the spectra of the hydrazine derivatives (5a, 5b, 5c, 5d, 6a, 6b, 6c, 7a,7b,7c, 7d) indicated the presence of amine (-NH2) peak had disappeared. Additionally, the acid protons (-OH) exhibited singlets between around 11.00 ppm to 12.00 ppm.

In their ^{13}C NMR spectra, compounds (5a, 5b, 5c, 5d, 6a, 6b, 6c, 7a,7b,7c, 7d), with amine (-N-CH) and carbonyl (-NH-CO-NH-) groups, showed signals at approximately 150.12 ppm and 158.1 ppm, respectively.
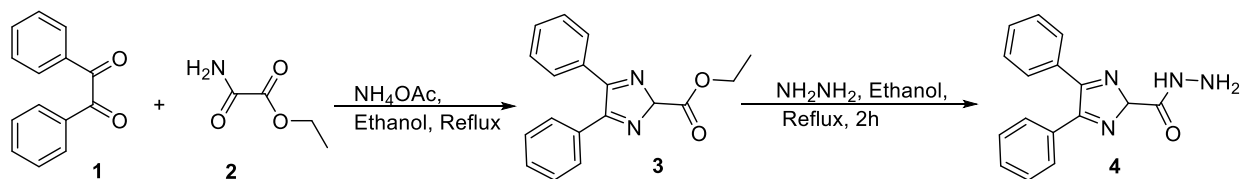
Scheme 1 Synthesis of key intermediate 4,5-diphenyl-2H-imidazole-2-carbohydrazide (**4**).
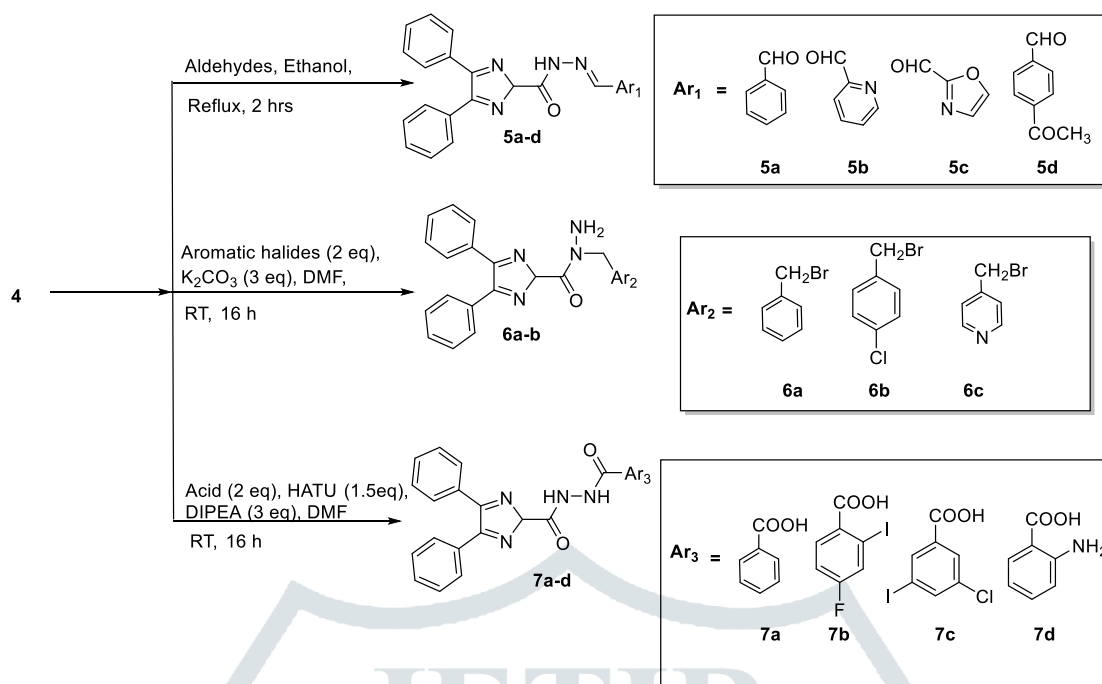
Scheme 2. Synthesis of designed compounds from intermediate **4**.

4.1 Conclusion

Among all synthesized derivatives, benzyl group bearing compound **7a** showed highest docking score. By this studies we understand the binding pattern of the active compound against enzyme acetyl Co-enzyme A. With this understanding, efforts are expended in our laboratory for further optimization of in-vitro and in-vivo activity.

4.2 Material and methods

4.2.1 Computational studies

The crystal structure of PA453A: acetyl CoA comples was fetched from the Protein Data Bank (PBD ID-51B0). The ligands preparations and energy minimizations were done using an MM2 force field with a minimum RMS gradient of 0.010 using Chem3D Pro 12.0. In-silico docking was performed using FBI reference ligand present in the raw PDB file and the same 3D-cordinates were used as grid coordinates for further exploration in the Auto Dock Vina. For the preparation of protein and to analyze the binding interactions Biovia Discovery Studio 2021, Pymol and Autodock Tools-1.5.6, were used. Missing residues in the protein structure were ignored as they didn't belong to the active sites; the binding affinity is remained unaffected. In the protein preparation step, the H_2O and hetero atoms were removed, and only-polar hydrogens were added to the receptor. In terms of charge neutralization, first Kollman charges were added followed by computing Gasteiger charge then the output file was saved in pdb format. 120 after the molecular docking all the compounds, the best compound 7a with docking score -10.3 kcal/mol found suitable and selected for the molecular dynamics simulation studies. Molecular dynamics simulation is an essential tool for the development of drug discovery. It is frequently used for the interactive studies and anlysis of the structural changes at the atomic level. A 5 nanoseconds (ns), MD simulation was performed and the final protein ligand complex trajectories was converted using the periodic boundary condition, which were used

to examine the conformational changes during the course of MD simulations. The root mean square deviation (RMSD) were used to examine the confirmational flexibilty in the receptor bind with the ligand. Compound **7a** interacted with all PAS residues through hydrophobic interactions (Tyr E:69, Tyr F:69 and Tyr F:38) and electrostatic interactions (Asp F:30 and Asp E:64). At the anionic subsite, compound 7a formed hydrophobic interactions with the Phe F:107 and MetF:60 and electrostatic interactions with the Glu F:29 residue. The N-atom of compound 7a interacted with the AspF:30 and GluF:29. At the oxyanion site, compound **7a** interacted with ArgE:66, as shown in figure 2.
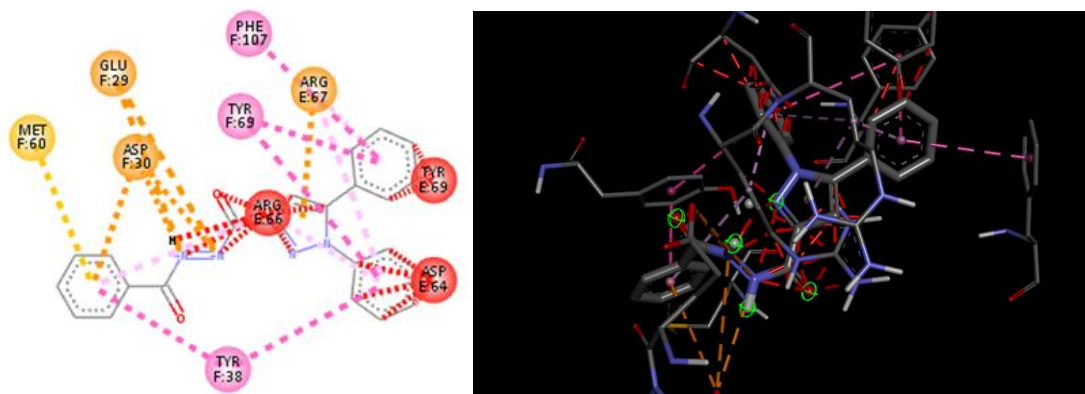
Figure 2. Docking of compound 7a in the AChE enzyme (A) Image of 3D interaction in the ligand binding. (B) 2D image showing the active site interactions.

5. *Experimental*

5.1 *Docking*

Molecular docking studies of designed compounds were carried out using computer aided drug design (CADD) approach by PyRx which is virtual screening software for computational drug discovery that can be used to screen libraries of compounds against potential drug targets. The ligand preparations and energy minimizations were done using an MM2 force field with a minimum RMS gradient of 0.010 on Chem 3D pro 12.0. In-silico docking was performed using FBI reference ligand present in the raw PDB file and the same 3D-co-ordinates were used as grid coordinate in the Auto Dock Vina. On the basis of MMPBSA.py which is a python-based script implemented in AMBER package that's allowed the individuals to perform quick and efficient calculations of free energy from MD simulations. The binding free energy can be estimated as follow:

$$\Delta G_{bind} = <G_{COMPL}> - <G_{RECEP}> - <G_{LIG}>$$
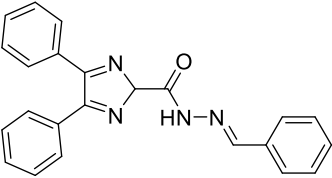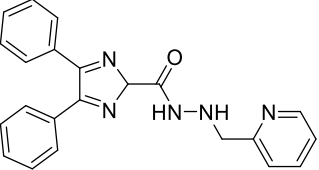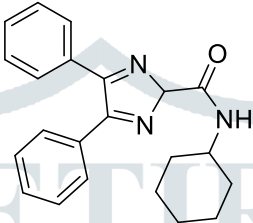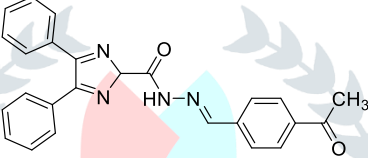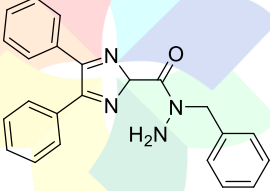
G_{COMPL} = free energy corresponding to the final complex;
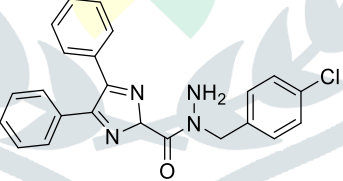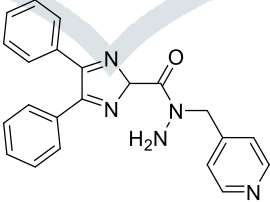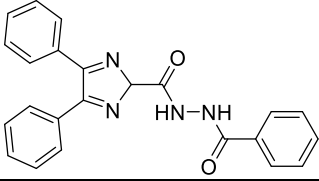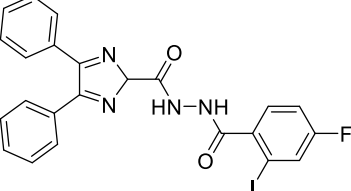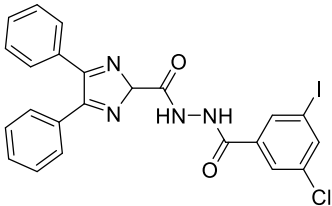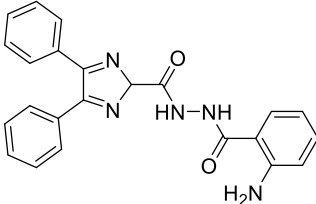
G_{RECEP} = free energy corresponding to the receptor only

G_{LIG} = free energy corresponding to the ligand only

The details of all synthesized compound and their binding pattern at the active site of receptor were successfully visualized with the help of software. Docking score of all the compounds is shown in the Table 1.

Table 1. Docking score of all synthesized compounds

S No.	Compound Code	Structure	Docking score
1	5a		-9.9
2	5b		-9.5
3	5c		-8.6
4	5d		-10
5	6a		-9.6
6	6b		-8.5
7	6c		-9.2
8	7a		-10.3
9	7b		-9.9

10	7c		-9.8
11	7d		-9.8

5.2 Chemistry

All solvents and chemicals used in this study were of analytical grade and purchased from Sigma-Aldrich, TCI chemicals and Avra Synthesis Pvt Ltd., India and were used without further purification. Progress of each reaction was monitored by TLC. ^{1}H NMR (400 MHz) spectra were recorded (Bruker Avance FT-NMR spectrophotometer, USA) in deuterated solvent (DMSO-d_6) using tetramethylsilane (TMS) as an internal standard; the chemical shifts (δ, ppm) and coupling constants (J, Hz) are reported. FT-IR spectra were recorded on an Alpha ECO-ATR Spectrophotometer (Bruker, USA).

5.2.1 Synthesis of ethyl 4,5-diphenyl-2H-imidazole-2-carboxylate (3)

Benzil **1** (10 g, 47.6 mmol, 1.0 eq) is reacted with ethyl 2-amino-2-oxoacetate **2** (8.35 g, 71.4 mmol, 1.5 eq) in the presence of ammonium acetate (18.35 g, 238 mmol, 5.0 eq) and ethanol at 80-85°C. The reaction mixture was stirred and refluxed for 3 h. The reaction mixture monitored by TLC and after completion reaction was evaporated under vacuum to get a solid material. Crude residue was washed with water and extracted with DCM and brine to get organic solvent. The combined organic phases were dried with anhydrous sodium sulfate, filtered and concentrated under vacuum at room temperature (RT) to afford the 4,5-diphenyl-2H-imidazole ester as 9.0 g (yield-65%) **(3)**.

MS (E1) MZ\value (M+1)- 292

^{1}H NMR (400 MHz, DMSO-d6): 9.50 (s, 1H), 7.42 (m, 3H), 7.34 (d, J=6.2 Hz, 5H), 7.21 (d, J=9.5 Hz, 2H), 7.01 (s, 1H), 4.2 (m, 4H), 1.20 (t, 3H).

5.2.2 Synthesis of 4,5-diphenyl-2H-imidazole-2-carbohydrazide (4)

Compound **3** (9.0, 30.8 mmol, 1.0 eq) was dissolved in absolute ethanol and stirred for 10 min followed by addition of 85% hydrazine hydrate (2.46 mL, 77.0mmol, 2.5 eq) in it. The reaction mixture was refluxed for 2 h to get white solid compound than cooled at room temperature. Then the solid was filtered and washed with absolute ethanol and dried under vacuum to get the 4,5-diphenyl-2H-imidazole-2-carbohydrazide 6.0 g, (yield-70%) **(4)**.

MS (E1) MZ\value (M+1)- 279.3

^{1}H NMR (400 MHz, DMSO-d6): 9.57 (s, 1H), 7.45 (m, 3H), 7.36 (d, J=6.2 Hz, 5H), 7.25 (d, J=9.6 Hz, 2H), 7.01 (s, 1H), 4.7 (d, J=3.2 Hz, 2H).

5.2.3 The general procedure of synthesis of compounds (5a-d)

Compound **4** (1.0 g, 3.5 mmol, 1.0 eq.) was dissolved in absolute ethanol (30 ml) at refluxing temperature followed by addition of substituted and substituted aromatic aldehyde (7.0 mmol, 2.0 eq) and 1-2 drop of acetic acid as catalyst. The reaction mixture was stirred and refluxed for 2 h. The reaction solution was cooled to get the solid compound then filtered and washed with ethanol. Solid compound was vacuum dried to get compounds (**5a-d**).

5.2.3.1 (E)-N'-benzylidene-4,5-diphenyl-2H-imidazole-2-carbohydrazide (5a)-
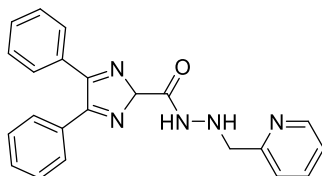
MS (E1) MZ\value (M+1)- 367.12

^{1}H NMR (400 MHz, DMSO-d6): 11.81 (s, 1H), 8.54 (s, 1H), 7.72 (d, J=8.8 Hz, 3H), 7.67 (m, 9H), 7.44 (m, 2H), 7.30 (s, 1H), 4.48 (d, J=5.6 Hz, 1H).
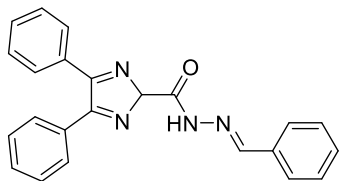
5.2.3.2 N'-benzyl-4,5-diphenyl-2H-imidazole-2-carbohydrazide (5b)-

MS (E1) MZ\value (M-1)- 368.1

1H NMR (400 MHz, DMSO-d_6): 11.94 (s, 1H), 9.64 (s, 1H), 8.04 (d, J = 6.9 Hz, 1H) 7.31 (m, 7H), 7.10 (m, 6H) 6.89 (s, 1H) 6.14 (d, J = 8.3 Hz, 2H).
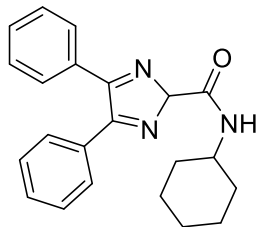

5.2.3.3 N-cyclohexyl-4,5-diphenyl-2H-imidazole-2-carboxamide (5c)-

MS (E1) MZ\value (M+1)- 346.1

1H NMR (400 MHz, DMSO-d6): 7.91 (d, J=8.4 Hz, 1H), 7.43 (m, 5H), 7.28 (m, 2H), 7.21 (d, J=6.8 Hz, 2H), 3.76 (m, 1H), 2.18 (s, 3H), 1.78 (m, 4H), 1.59 (m, 1H), 1.33 (m, 4H), 1.11 (m, 1H).
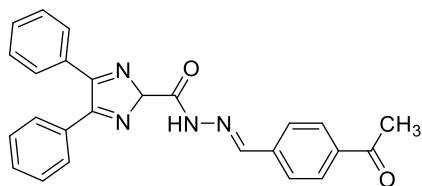
IR (v, cm-1): 3279.36 (N-H stretch), 2854.67 (alkane, C-H), 1634.70 (amide, C=O), 1547.84 (alkene, C=C), 1357.67 (C-H bending).

m.p- 240-241°C.

5.2.3.4 (E)-N'-(4-acetylbenzylidene)-4,5-diphenyl-2H-imidazole-2-carbohydrazide (5d)-
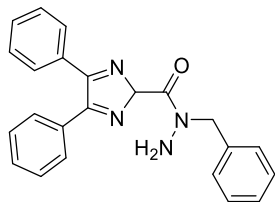
MS (E1) MZ\value (M+1)- 409.12

5.2.4 The general procedure of synthesis of compounds (6a-c)

Compound **4** (1.0 g, 3.5 mmol, 1.0 eq) was dissolved in the DMF (10 mL) solvent in the presence of various aromatic halides (5.5 mmol) and anhydrous potassium carbonate (17.5 mmol). Reaction mixture was stirred at room temperature for 16 h. Monitored reaction by TLC, after starting material (SM) consumed. The reaction mixture was evaporated under vacuum at 45-50°C to get a crude residue and which was washed with water and extracted with ethyl acetate and brine to collect the organic phase. The combined organic phases were dried with anhydrous sodium sulfate, filtered and concentrated in vacuum to give compounds (**6a-c**).

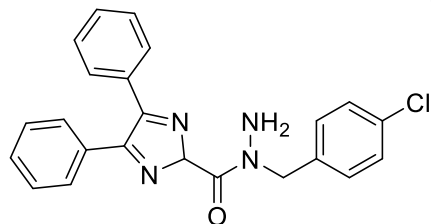### 5.2.4.1 2-amino-1-(4,5-diphenyl-2H-imidazol-2-yl)-2-(phenylamino)ethan-1-one (6a)-

MS (E1) MZ\value (M+1)- 369.12

^{1}H NMR (400 MHz, DMSO-d6): 11.81 (s, 1H), 8.54 (s, 1H), 7.72 (d, J=8.8 Hz, 3H), 7.67 (m, 11H), 7.30 (s, 1H), 4.48 (d, J=5.6 Hz, 1H).

5.2.4.2 2-amino-2-((4-chlorobenzyl)amino)-1-(4,5-diphenyl-2H-imidazol-2-yl)ethan-1-one (6b)-
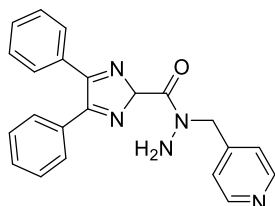
MS (E1) MZ\value (M+1)- 403.2

5.2.4.3 N,N'-bis(4-chlorobenzyl)-4,5-diphenyl-2H-imidazole-2-carbohydrazide (6c)-

MS (E1) MZ\value (M-1)- 368.2

^{1}H NMR (400 MHz, DMSO-d6): 9.38 (s, 1H), 7.49 (d, J=8.4 Hz, 5H), 7.41 (d, J=4.4 Hz, 37.H), 7.30 (m, 10H), 7.19 (d, J=5.6 Hz, 2H), 6.88 (s, 1H).

5.2.5 Synthesis of 4,5-diphenyl-N'-(pyridin-2-ylmethyl)-1H-imidazole-2-carbohydrazide (7a-7d)-

Substituted aromatic acid (3.5 mmol) was dissolved in DMF (30 ml) at room temperature followed by addition of HATU (7.0 mmol), and DIPEA (17.5 mmol). Then compound **4** (3.5 mmol) was added into the reaction and stirred at room temperature for 16 hrs. Reaction monitored by TLC after reaction completion, reaction solution was filtered and concentrated in vacuum and purified using the column chromatography to get compounds **(7a-7d)**.
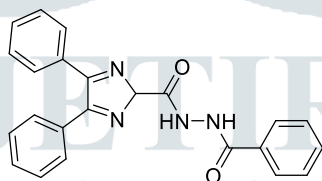
5.2.5.1 N'-benzoyl-1,5-diphenyl-1H-pyrazole-3-carbohydrazide (7a)-

MS (E1) MZ\value (M+1)- 383.1

^{1}H NMR (400 MHz, DMSO-d6): 10.49 (s, 1H), 10.34 (s, 1H), 7.92 (d, J=7.6 Hz, 5H), 7.59 (d, J=6.4 Hz, 1H), 7.52 (m, 5H), 7.46 (d, J=7.2 Hz, 5H), 7.34 (m, 2H), 7.11 (s, 1H).

IR (v, cm-1): 3249.8 (N-H stretch), 3055 (alkane, C-H), 1636.29 (amide, C=O), 1553.76 (alkene, C=C), 1367.31 (C-H bending), 1230.57 (Ar-C-N).
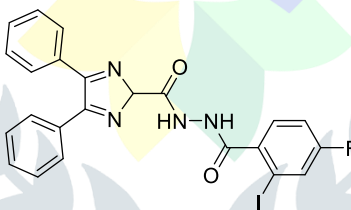
m.p- 189-190°C.

5.2.5.2 N'-(4-fluoro-2-iodobenzoyl)-1,5-diphenyl-1H-pyrazole-3-carbohydrazide (7b)-
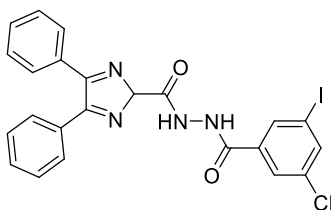
MS (E1) MZ\value (M+1)- 527.0

^{1}H NMR (400 MHz, DMSO-d6): 10.5 (s, 1H), 10.1 (s, 1H), 7.49 (d, J=8.4 Hz, 5H), 7.41 (d, J=4.4 Hz, 37.H), 7.30 (m, 10H), 7.19 (d, J=5.6 Hz, 2H), 6.88 (s, 1H).

5.2.5.3 N'-(3-chloro-5-iodobenzoyl)-4,5-diphenyl-2H-imidazole-2-carbohydrazide (7c)-

MS (E1) MZ\value (M+1)- 543.1

^{1}H NMR (400 MHz, DMSO-d6): 10.69 (s, 1H), 10.45 (s, 1H), 8.22 (t, J=2.8 Hz, 1H), 8.11 (s, 1H), 7.95 (m, 1H), 7.47 (m, 5H), 7.38 (m, 2H), 7.11 (s, 1H).
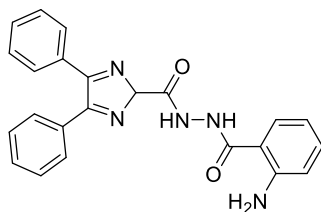

5.2.5.4 (E)-((2-aminobenzoyl)diazenyl)(4,5-diphenyl-2H-imidazol-2-yl)methanone (7d)-

MS (E1) MZ\value (M+1)- 396.12

IR (v, cm-1): 3220.05 (N-H stretch), 1639.07 (amide, C=O), 1528.01 (alkene, C=C), 1368.63 (C-H bending), 1243.95 (Ar-C-N).

m.p- 127-128 °C.

Acknowledgements

References

1. Berman, H.M.; Westbrook, J.; Feng, Z; Gilliland, G.; Bhat, T.N.; Weissig, H.; Shindyalov, I.N.; Bourne, P.E. 2000. The Protein Data Bank. http://www.rcsb.org/pdb/status.html.

2. Allinger, N.L. Conformational Analysis.130.MM2. A Hydrocarbon Force Field Utilizing V I and V2 Torsional Terms1j2, n.d.

3. Trott, O.; Olson, A.J. 2009. AutoDockVina: Improving the speed and accuracy of docking with a new scoring function, efficient optimization, and multithreading. J Comput Chem. NA. https://doi.org/10.1002/jcc.21334.

4. BIOVIA, Dassault Systems, Biovia Discovery Studio 2021. (n.d.).

5. Delano, W.L. 2000. The PyMOL Molecular Graphics System.

6. Morris, G.M.; Huey, R.; Lindstrom, W.; Sanner, M.F.; Belew, R.K.; Goodsell, D.S.; Olson, A.J. 2009. AutoDock4 and AutoDockTools4: Automated docking with selective receptor flexibility. J Comput Chem. 30, 785-2791. https://dio.org/10.1002/jcc.21256.

7. Wang, J.; Cieplak, P.; Kollman, P.A. 2000. How Well Does a Restrained Electrostatic Potential (RESP) Model Perform in Calculating Conformational Energies of Organic and Biological Molecules. J Comput Chem. 21, 1049-1074. https://doi.org/10.1002/1096-987X(200009)21:12<1049::AID-JCC3>3.0.CO;2-F.

8. Abraham, M.; Alekseenko, A.; Bergh, C.; Blau, C.; Briand, E.; Doijade, M.; Fleischmann, S.; Gapsys, V.; Garg, G.; Gorelov, S.; Gouaillardet, G.; Gray, A.; Irrgang, M.E.; Jalalypour, F.; Jordan, J.; Junghans, C.; Kanduri, P.; Keller, S.; Kutzner, C.; Lemkul, J.A.; Lundborg, M.; Merz, P.; Miletic, V.; Morozov, D.; Pall, S.; Schulz, R.; Shirts, M.; Shvetsov, A.; Soproni, B.; Van, D.; Spoel, D.; Turner, P.; Uphoff, C.; Villa, A.; Wingbermuhle, S.; Zhmurov, A.; Bauer, P.; Hess, B.; Lindahl, E. 2023. GROMACS 2023 Source code. https://doi.org/10.5281/zenodo.7588619.

9. Silva, D.; Vranken, B.F. 2012. ACPYPE-Ante Chamber Python Parser interface. http://www.biomedcentral.com/1756-0500/5/367.

10. Wang, J.; Wolf, R.M.; Caldwell, J.W.; Kollman, P.A.; Case, D.A. 2004. Development and testing of general amber force field. J Comput Chem. 25, 1157-1174. https://doi.org/10.1002/jcc.20035.

11. Wang, J.; Wang, W.; Kollman, P.A.; Case, D.A. 2006. Automatic atom type and bond type perception in molecular mechanical calculations. J Mol Graph Model. 25, 247-260. https://doi.org/10.1016/j.jmgm.2005.12.005.

12. Varshney, A.P.; Brooks, F.; William, J.V. 1994. Linearly Scalable Computation of Smooth Molecular Surfaces.

13. Frishman, D.; Argos, P. 1995. Knowledge-based protein secondary structure assignment, proteins: Structure, Function, and Genetics. 23, 566-579. https://doi.org/10.1002/prot.340230412.

14. Theses, M.; Stone, J.E. 1998. Scholars' Mine Scholars' Mine An efficient library for parallel ray tracing and animation, an efficient library for parallel ray tracing and animation. https://scholarsmine.mst.edu/masters_theseshttps://scholarsmine.mst.edu/masters_theses/1747.

15. Eargle, J.; Wright, D.; Luthey-Schulten, Z. 2006. Multiple Alignment of protein structures and sequences for VMD. Bioinformatics. 22, 504-506. https://doi.org/10.1093/bioinformatics/bti825.

16. Stone, J.E.; Gullingsrud, J.; Schulten, K. 2001. A system for interactive molecular dynamics simulation, in proceedings of the 2001 Symposium on Interactive 3D Graphics –SI3D'01. ACM Press, New York, New York, USA. pp. 191-194. https://doi.org/10.1145/364338.364398.

17. Humphrey, W.; Dalke, A.; Schulten, K. 1996. VMD:Virtual Molecular Dynamics. Journal of Molecular Graphics. 14, 33-38.

18. Sanner, M.F.; Olson, A.J.; Spehner, J.C. 1995. Fast and robust computation of molecular surfaces, in: proceedings of the Eleventh Annual Symposium on Computational Geometry –SCG'95. ACM Press, New York, New York, USA. pp. 406-407. https://doi.org/10.1145/220279.220324.

19. Sharma, R.; Zeller, M.; Pavlovic, V.I.; Huang, T.S.; Lo, Z.; Chu, S.; Zhao, Y.; Phillips, J.C.; Schulten, K. 2000. Speech/gesture interface to a visual-computing environment, IEEE Comput Graph Appl. 20, 29-37. https://doi.org/10.1109/38.824531.

20. Miller, B.R. 3rd. McGee, T.D.; Swails, J.M.; Homeyer, N.; Gohlke, H.; Roitberg, A.E. 2012. MMPBSA.py: an Efficient Program for End-State Free Energy Calculations. J Chem Theory Comput. 8, 3314-3321. https://doi.org/10.1021/ct300418h.

21. Valdes-Tresanco, M.S.; Valiente, A.E.; Moreno, E. 2021. Gmx MMPBSA: A New Tool to Perform End-State Free Energy Calculations with GROMACS. J Chem Theory Comput. 17, 6281-6291. https://doi.org/10.1021/acs.jctc.1c00645.

22. Bondi, A. 1964. Van der Waals Volumes and Radii, J Phys Chem. 68, 441-451. https://doi.org/10.1021/j100785a001.

23. Aksungur, P. A.; Sungur, S.; Ünal, A. B.; Iskit, C. A.; Squier. and S. Şenel. 2004. "Chitosandelivery

systems for the treatment of oral mucositis: in vitro and in vivo studies."Journalofcontrolledrelease **98**(2):269-279.

24. Nascimento. I. J. D. S.; Aquinol, T. M. D.; Silva junior, E. F. D. 2022. The New Era of Drug Discovery: The Power of Computer-aided Drug Design (CADD). Letters in Drug Design & Discovery. 19, 951-955.

25. Mandal, S.; Moudgil, M.; Mandal, S. K. 2009. Rational drug design. European Jornal of pharmacology. Volume 625, Issues 1-3, 90-100.

26. Huggins, D. J.; Sherman, W.; Tidor, B. 2012. Rational approaches to improving selectivity in drug design. J. Med. Chem, 55, 1424-1444.

27. Reddy. M. R.; Parrill, A. L. 1999. Overview of rational drug design. ACS publication.

28. Ramirez, D. 2016. Computational Methods Applied to Rational Drug Design. The Open Medicinal Chemistry Journal. 10, 7-20. DOI: 10.2174/1874104501610010007.

29. Kitson, S. L. 2017. Squaryl molecular metaphors- Application to rational drug design and imaging agents. Journal of diagnostic imaging in therapy. 4(1): 35-75.

30. Eliezer, L. M. L. and Barreiro, J. 2005. Bioisosterism: A Useful Strategy for Molecular Modification and Drug Design. Current Medicinal Chemistry. 12, 23-49.

31. Meanwell. N.A. 2013. The Influence of Bioisosteres in Drug Design: Tactical Applications to Address Developability Problems. Top Med Chem.

32. Patani. G. A and Lavoie. E. J. 1996. Bioisosterism: A rational approaches in drug design. Chem. Rev. 96, 3147-3176.

33. Ramarao, S. P.; Verma, A.; waiker, D. K.; Tripathi, P. N.; Shrivastava, S. K. 2021. Design, synthesis and evaluation of some novel biphenyl imidazole derivatives for the treatment of Alzheimers disease. Journal of molecular structure 1246. 131152.